Spectroscopic and reaction mechanism implications from ^{164}Dy(d, t)^{163}Dy and ^{166}Er(d, t)^{165}Er measurements*

J. V. Maher, H. S. Song, G. H. Wedberg, and J. L. Ricci
University of Pittsburgh, Pittsburgh, Pennsylvania 15260
(Received 22 March 1976)

Angular distributions have been measured for transitions populating residual states of ^{163}Dy and ^{165}Er through the (d,t) reaction at $E_d = 17$ MeV. Many of these angular distributions have shapes which are well reproduced by distorted wave Born approximation calculations which assume orbital angular momentum transfers l which are compatible with the previously assigned spin-parities of the states. But a significant number of angular distributions are anomalous; i.e., either they cannot be fitted by any reasonable distorted wave Born approximation calculation or they can only be fitted with a calculation which assumes an l value incompatible with the previous Nilsson model assignment of the state. While the summed spectroscopic factors are in good agreement with Nilsson model expectations, there is considerable evidence of fragmentation of single-quasihole strength (most dramatically for ^{164}Dy→^{163}Dy $l = 0$ transitions, 12 of which are observed) and the spectroscopic factors for several levels deviate significantly from Nilsson model predictions, even though Coriolis coupling has been included in the model calculation. This observation of several strongly anomalous angular distributions, along with large discrepancies between observed and model-predicted spectroscopic factors, almost certainly indicates that the assumption of a simple one-step direct reaction mechanism breaks down for some of these transitions. No evidence is found to indicate the position of the (expected strongly populated) $7/2^+[404]$ state. Several other possible changes in previous Nilsson model assignments are indicated.

[NUCLEAR REACTIONS ^{164}Dy(d,t), ^{166}Er(d,t), $E_d = 17$ MeV measured $\sigma(\theta)$; DWBA analysis, deduced levels, l values, spectroscopic factors. Enriched targets.]

I. INTRODUCTION

The limits of applicability of direct reaction assumption are not well established and the investigation of these limits has motivated many recent investigations.[1-3] Unfortunately, since distorted wave Born approximation (DWBA) calculations are easily performed and the next most reasonable improvement—the coupled-channels Born approximation (CCBA) calculation—is much more difficult to perform, there has been a tendency to vary parameters to fit as much data as possible with DWBA and to apply CCBA only in an *ad hoc* fashion to troublesome cases of experimental data. This difficulty in defining the limits of applicability of the DWBA is exacerbated by problems of acquiring a data base. Multinucleon transfer reactions frequently stretch the DWBA assumptions, but for such reactions it is not possible to separate structure from kinematic factors in the DWBA calculations so the analysis procedure is less reliable than for single-nucleon transfer reactions where structure and kinematic factors are algebraically separable. On the other hand, multistep effects in single-nucleon transfer reactions appear to be small for most cases of spherical nuclides.[4] The study of (d,t) reactions on deformed rare-earth targets provides an excellent opportunity to acquire an extensive set of data for which the DWBA assumptions should be marginal and for which the DWBA analysis should be reasonably straightforward. Both the deuteron and the triton are strongly absorbed and at least for most transitions in spherical nuclides, (d,t) angular distributions are smooth diffraction patterns which are easily fitted with DWBA calculations that use reasonable optical model parameter sets. The splittings of single-particle states in deformed nuclei provides, in any one deformed residual nucleus, a multiplicity of states of each spin, in most of which the amplitudes for population by direct single-particle transfer are sufficiently small that multistep effects might be detectable.[5,6]

This work is part of a larger investigation into the spectroscopy of the deformed rare-earth region and the mechanism of the (d,t) reaction in this mass region. In one previous paper[7] it was shown that, when the (d,t) reaction is initiated by 17 MeV deuterons, the angular distribution shapes are unambiguously characteristic of orbital angular momentum transfer (l) over the entire range $0 \leq l \leq 6$. Another report[8] of part of this series of investigations presented evidence for systematic violations of one-step direct reaction assumptions in certain single-particle states in the even-even targets ^{160}Gd, ^{162,164}Dy, and ^{166,168}Er, i.e., DWBA analysis of the observable transitions to members of the $\frac{11}{2}^-[505]$, $\frac{3}{2}^-[521]$, $\frac{1}{2}^-[521]$, and $\frac{5}{2}^+[642]$ Nilsson

bands shows anomalous spectroscopic factors and/or anomalous angular distribution shapes for transitions to some members of each of these bands in nearly all residual nuclides which were studied. The transitions discussed in Ref. 8 were restricted to low-lying states of reasonably well established spin-parity where there is no doubt of expected orbital angular momentum transfer (l) and where unaccounted vibrational couplings should have minimum effects on Nilsson model predictions of single-particle strengths. A recent paper[9] in this series presented both reaction mechanism and spectroscopic results for all the observed transitions in a study of the (d,t) reaction on the $N=96$ isotones ^{160}Gd and ^{162}Dy. In addition to showing several anomalous angular distributions, principally for transitions to members of the above-mentioned rotational bands, angular distributions presented in Ref. 9 for several transitions to levels in ^{159}Gd and ^{161}Dy are characteristic of l values inconsistent with the previous Nilsson model assignment of the residual state. The most notable of these suggested changes in assignment of single-particle states erases both previous assignments of the positions in ^{159}Gd and ^{163}Dy of the $\frac{7}{2}^+[404]$ bandhead, thus raising a question as to where this strong hole state should appear.

This paper presents the detailed results of an investigation of the (d,t) reaction at 17 MeV on the $N=98$ isotones ^{164}Dy and ^{166}Er. Individual (d,t) spectra have been measured for each of these nuclei[10-12] at lower beam energy (12 MeV). No angular distributions have previously been reported. ^{163}Dy has also been studied through Coulomb excitation,[13] through (n,γ)[10] and γ decay following ^{163}Tb electron capture,[14] and through its population in ^{164}Dy(^{3}He, α) spectra.[15] ^{165}Er has previously been studied through γ decays following several kinds of reaction,[16-19] through electron capture,[20] and through its population in (^{3}He, α) spectra.[21]

The data of the present investigation have been analyzed with finite range nonlocal DWBA calculations. The intent of this analysis is to organize the data for comparison with Nilsson model expectations as to orbital angular momentum transfer (l) and spectroscopic strength. Since, between the Nilsson model and the DWBA calculations, there are many possible parameters which could be varied, an attempt has been made to standardize the analysis parameters with the best available information rather than make *ad hoc* parameter variations to fit data for individual transitions. The selection of parameters is discussed for the DWBA calculations in Sec. III and for the calculations of Nilsson model spectroscopic factors in Sec. IV. It has not been possible to perform CCBA calculations, but it is hoped that the present results will provide a reasonable extensive data base for CCBA calculations to investigate under what spectroscopic/reaction dynamic conditions the assumption of a one-step direct transfer mechanism breaks down.

II. DATA ACQUISITION AND REDUCTION

The experiment was performed with 17 MeV deuterons from the Pittsburgh three stage Van de Graaff accelerator. The targets were ~100 μg/cm^2 foils of metallic Dy (enriched to 98.4% ^{164}Dy) and Er (enriched to 94.9% ^{166}Er) evaporated on carbon backings. Tritons from the (d,t) reaction were detected in photographic emulsions placed in

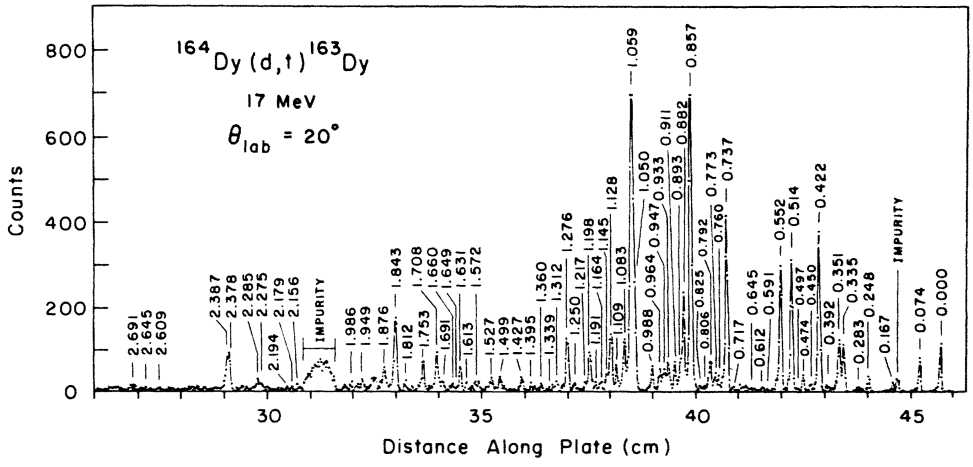

FIG. 1. Spectrum of tritons from the ^{164}Dy$(d,t)^{163}$Dy reaction measured at $\theta_{lab}=20°$. Excitation energies of residual states are listed in MeV.

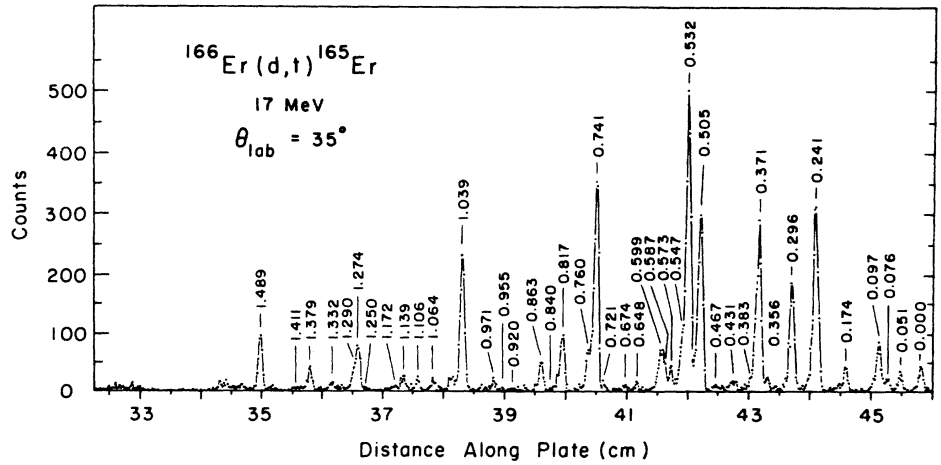

FIG. 2. Spectrum of tritons from the ^{166}Er$(d,t)^{165}$Er reaction measured at $\theta_{lab} = 35°$. Excitation energies of residual states are listed in MeV.

the focal plane of a split-pole spectrograph. The spectrograph entrance aperture subtended a solid angle of 1.4 msr. The developed photographic plates were scanned by the Argonne automatic plate scanner[22]; some were checked by human scanners. Typical spectra are shown in Figs. 1 and 2. The energy resolution was ~9 keV for the ^{164}Dy(d,t) ^{163}Dy reaction and ~12 keV for the ^{166}Er (d,t) ^{165}Er reaction. Measurements were made for the Dy reaction at 13 angles over the

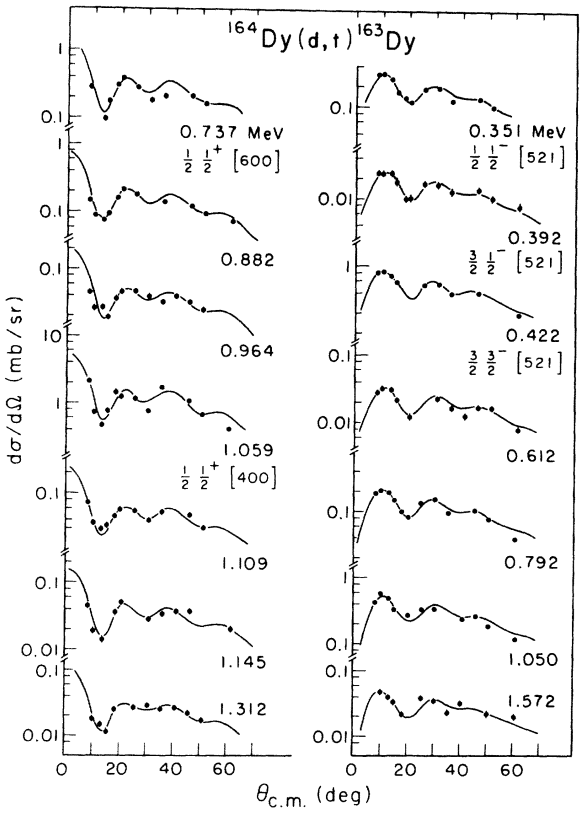

FIG. 3. $l = 0$ (left side) and $l = 1$ (right side) angular distributions from the ^{164}Dy$(d,t)^{163}$Dy reaction. The solid curves are DWBA calculations.

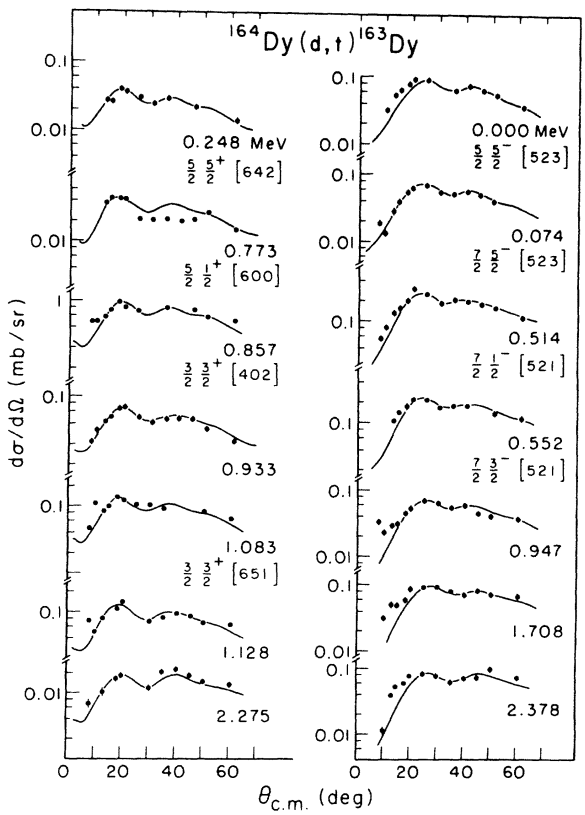

FIG. 4. $l = 2$ (left side) and $l = 3$ (right side) angular distributions from the ^{164}Dy$(d,t)^{163}$Dy reaction. The solid curves are DWBA calculations.

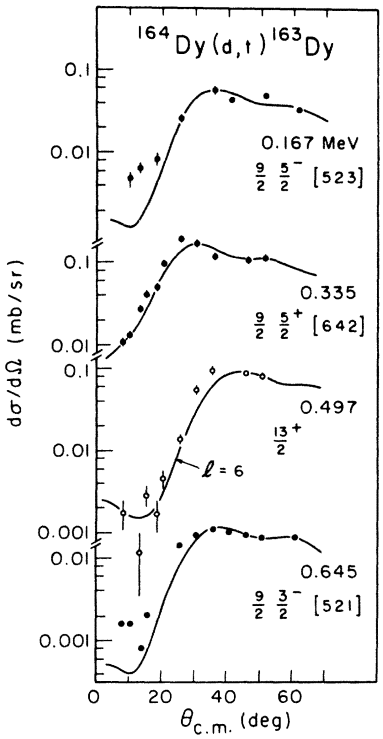

FIG. 5. $l \geq 4$ angular distributions from the ^{164}Dy$(d,t)^{163}$Dy reaction. The solid curves are DWBA calculations.

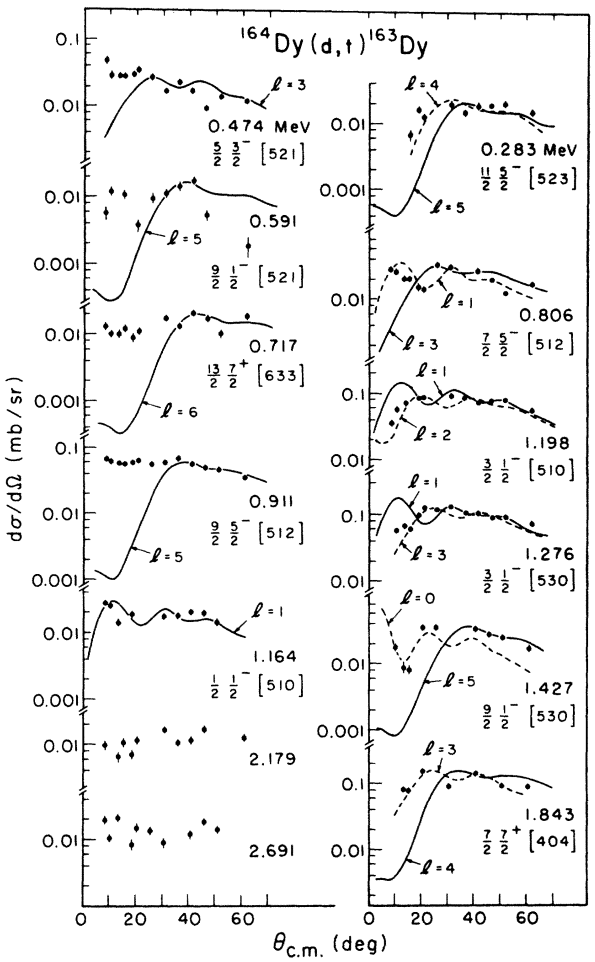

FIG. 6. Anomalous angular distributions from the ^{164}Dy$(d,t)^{163}$Dy reaction. Those on the left side cannot be fitted with any DWBA calculation. Those on the right can only be fitted by assuming an l value which is inconsistent with the previous Nilsson model assignment of the state.

range $8° \leq \theta_{lab} \leq 60°$ and for the Er reaction at 19 angles over the range $8° \leq \theta_{lab} \leq 65°$. Two NaI detectors were set at $\theta_{lab} = \pm 38°$ to monitor possible target deterioration (none of which was observed). Peak areas were extracted from the spectra with the peak-fitting code AUTOFIT.[23] The reliability of the fitting procedure was monitored with numerous hand checks.

Angular distributions have been measured for the elastic scattering of 17 MeV deuterons from ^{164}Dy, ^{166}Er, and other rare-earth targets [these and the results of an optical model analysis have been reported previously along with the results of the ^{160}Gd and ^{162}Dy(d,t) reactions[9]]. Since the elastic scattering cross sections were thus established, the yields from the NaI monitor detectors were used to extract the absolute cross sections of the (d,t) transitions. These absolute cross sections are expected to be accurate to ±15%. A representative selection from the many ^{164}Dy(d,t) ^{163}Dy angular distributions is shown in Figs. 3–6 and all ^{166}Er(d,t) ^{165}Er angular distributions are shown in Figs. 7–10.

III. DWBA CALCULATIONS AND ANGULAR DISTRIBUTION SHAPES

The code DWUCK[24] was used to perform the finite range nonlocal DWBA calculations described in this section. Table I lists the optical potential parameters and bound state potential parameters used in these calculations. The finite range parameter was set at 0.845 and nonlocality parameters at 0.54 (for the deuteron) and 0.25 (for the triton). The triton optical parameters are those of Flynn *et al.*[25] Two sets of deuteron optical potential parameters are listed in Table I. The first set resulted from a global fit to deuteron scattering (mostly on spherical nuclei) by Perey and Perey.[26] The second set resulted from the previously reported[9] fit to elastic scattering of 17 MeV deuterons from Dy and Er isotopes. This second potential is matched in shape to the triton potential and its well depth is near optimum to provide proper potential matching.[27] No significant differences were found between DWBA calculations performed

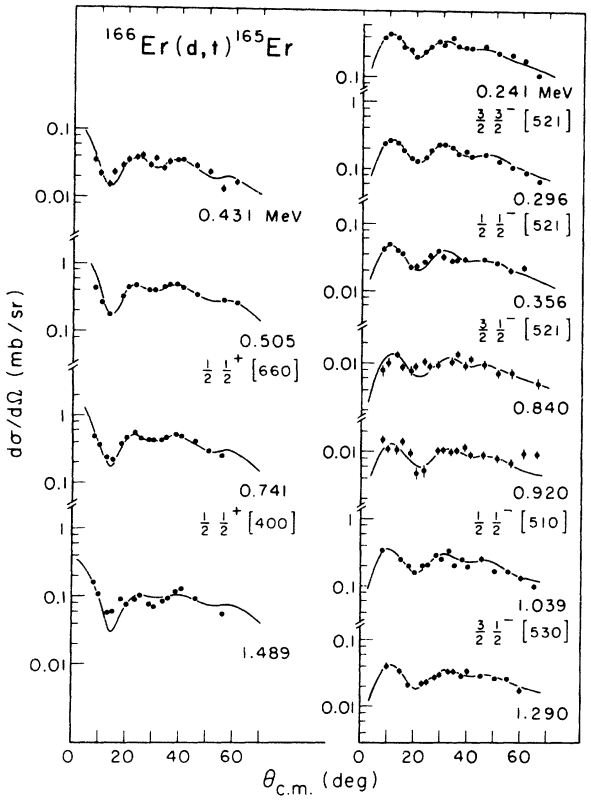

FIG. 7. $l=0$ (left side) and $l=1$ (right side) angular distributions from the ^{166}Er$(d,t)^{165}$Er reaction. The solid curves are DWBA calculations.

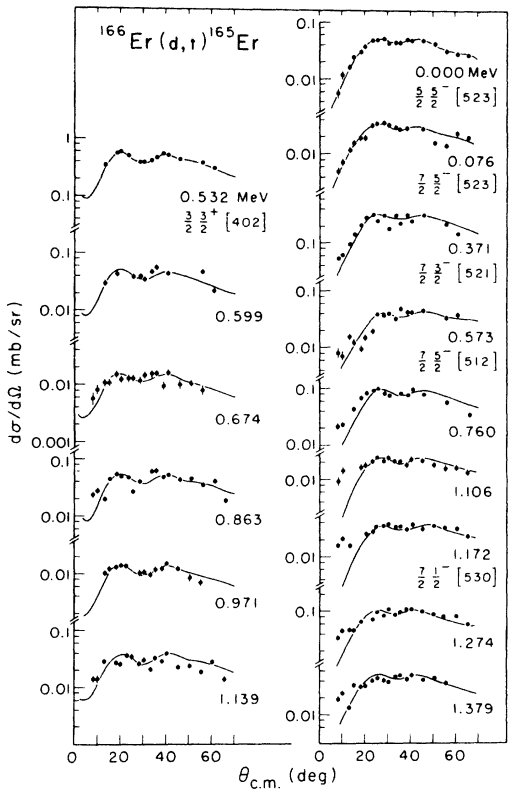

FIG. 8. $l=2$ (left side) and $l=3$ (right side) angular distributions from the ^{166}Er$(d,t)^{165}$Er reaction. The solid curves are DWBA calculations.

with the two deuteron potentials. All spectroscopic information presented below was extracted with DWBA calculations which used the Perey potential.

Some of the transitions of interest in this experiment involve total angular momentum values which, when used with the binding energy prescription in DWBA calculations, result in unreasonably shallow or deep bound state well depths (depending on which radial quantum number n is selected). This is a well known problem which occurs in spherical nuclei for states of weak single-particle (or -hole) character far separated from the centroid of their subshell.[28] The problem is more severe in deformed nuclei because the single-particle fragmentations that result from breaking spherical symmetry can place significant single-particle strength in an orbital whose binding energy is very different from that of the nearest spherical model orbital of the same spin and parity. Since DWBA expectations are known to have weak dependence on total angular momentum transfer (j), the experimental angular distributions have been fitted with the proper orbital angular momentum transfer (l) but with n and j values which keep the potential well depth in the bound state calculation near 60 MeV. Table II lists the nlj values employed in this analysis. With this procedure bound state well depths were always reasonable.

Angular distributions for most of the strong transitions observed in this experiment are well fitted by the DWBA calculations—as can be seen from Figs. 3–5 and 7–9. The strong $l=0$ and 1 angular distributions are extremely well fitted (Figs. 3 and 7). $l=2$ and $l=3$ angular distributions (Figs. 4 and 8) are also well fitted but with a tendency to have small angle cross sections larger than DWBA predictions. Higher l (≥ 4) transitions (Figs. 5 and 9) pose a problem. In this and previous experiments these transitions have frequently been very well fitted by DWBA calculations, but equally often the data deviate significantly from the DWBA prediction. This can be partially explained in a number of ways: (1) High l transitions are of intrinsically smaller cross section than are low l transitions so any contamination of the process with multistep effects might be expected to produce more dramatic results. (2) The first maximum in high l transfer DWBA angular dis-

tributions falls at a large angle. Since angular distributions are normally expected to drop steeply at angles smaller than this maximum, it is easier to identify deviations in high l transfer cases than for low l transfers where the small angle data points fall on or near the first DWBA maximum.

Figures 6 and 10 contain anomalous angular distributions. Some of these can be fitted by DWBA calculations for an l different from that required by the previously reported Nilsson model assignment of the level. This suggests that some of the anomalies can be attributed to misassignments in previous work, but in many cases DWBA calculations cannot fit the angular distribution for any l value.

IV. SPECTROSCOPIC FACTORS AND NILSSON MODEL PARAMETERS

Spectroscopic factors have been extracted from the measured angular distributions by using the relation:

$$\left(\frac{d\sigma}{d\Omega}\right)_{\text{exp}} = 3.33 C^2S \frac{(d\sigma/d\Omega)_{\text{DWBA}}}{(2j+1)},$$

where C^2S is the spectroscopic factor, $(d\sigma/d\Omega)_{\text{exp}}$ is the data, $(d\sigma/d\Omega)_{\text{DWBA}}$ is the DWBA calculation made with the code DWUCK, and j is the angular momentum transfer assumed in the calculation. Tables III and IV list, for each level populated in ^{163}Dy and ^{165}Er, excitation energy, the empirically determined l value, the Nilsson model assignment (where known from previous work), cross section at one angle, and spectroscopic factor. For those levels whose angular distributions show significant deviations from DWBA predictions but whose l values have been suggested from previous Nilsson model assignments or tentatively determined from the angular distribution shape, spectroscopic factors have been extracted and listed in Tables III and IV; but these spectroscopic factors are clearly uncertain, representing a normalization of the DWBA prediction to the measured cross section in the angular region of the principal maximum in the DWBA angular distribution. As is discussed below and in the Introduction, the DWBA is used in these cases to help organize the data with no strong claim of validity for resulting spectroscopic implications.

Also shown in Tables III and IV are spectroscopic factors predicted by Nilsson model calculations[29]

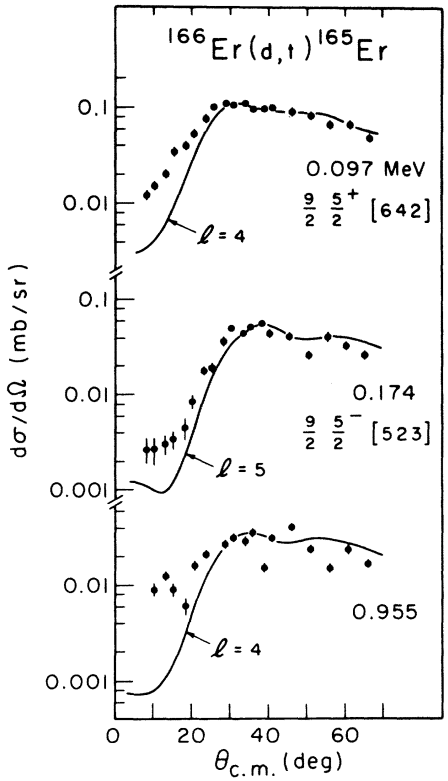

FIG. 9. $l \geq 4$ angular distributions from the ^{166}Er$(d,t)^{165}$Er reaction. The solid curves are DWBA calculations.

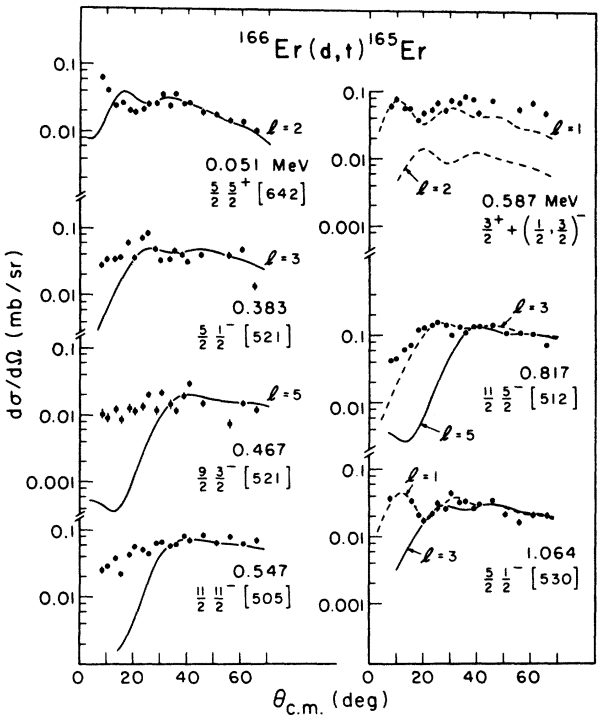

FIG. 10. Anomalous angular distributions from the ^{166}Er$(d,t)^{165}$Er reaction. Those on the left side cannot be fitted with any DWBA calculations. Those on the right can only be fitted by assuming an l value which is inconsistent with the previous Nilsson model assignment of the state.

TABLE I. Optical model parameters in the DWBA calculation and the bound state well parameters.

	V (MeV)	r_0 (fm)	r_0 (fm)	a (fm)	W (MeV)	W_D (MeV)	r_I (fm)	a_I (fm)	$\lambda_{s.o.}$
^{166}Er, ^{164}Dy+d [a]	102.2	1.15	1.15	0.81	···	17.6	1.34	0.68	···
^{166}Er, ^{164}Dy+d [b]	98.4	1.16	0.74	0.752	10.4	···	1.48	0.957	···
^{165}Er, ^{163}Dy+t [c]	166.7	1.16	1.40	0.752	14.7	···	1.498	0.817	···
Bound states	d	1.25	1.25	0.65					

[a] Reference 26.
[b] Reference 9.
[c] Reference 25.
[d] Adjusted to give correct separation energy.

performed with the code BANDFIT.[30] Given an energy spectrum with spin, parity, and Nilsson model quantum numbers assigned to each level, this code will vary any or all of several parameters to fit the energy spectrum and then use the resulting parameters to predict spectroscopic factors for single-nucleon transfer reactions. As BANDFIT was used in this investigation, the parameters of the Nilsson deformed well were fixed at $\beta = 0.30$, $\mu = 0.42$, and $\kappa = 0.0637$. The orbital emptiness parameters (or pairing factors V^2) were constrained to satisfy the relation

$$V_i^2 = \frac{1}{2}\left(1 - \frac{\epsilon_i - \lambda}{[(\epsilon_i - \lambda)^2 + \Delta^2]^{1/2}}\right),$$

where $\epsilon_i - \lambda$ is the difference between the single-particle energy ϵ_i of the ith Nilsson orbital and the Fermi energy λ, and Δ is the pairing gap (which was taken from odd-even mass differences). The V_i^2 were determined by identifying bandhead energies, after subtraction of rotational energy, with quasiparticle energies $\{[(\epsilon_i - \lambda)^2 + \Delta^2]^{1/2} - \Delta\}$. The bandhead energies, moment of inertia parameters, and, for $K = \frac{1}{2}$ bands, the decoupling parameters were varied in the fitting procedure. As has been noted previously,[31] best results were obtained by reducing Coriolis coupling matrix elements to 60% of the value calculated by the Nilsson model. Table V lists the final values of bandhead energies, moment of inertia parameters, and decoupling parameters along with the orbital emptiness parameters for all the Nilsson levels considered.

The BANDMIX code further used the Nilsson model parameters determined by the above procedure to calculate spectroscopic factors

$$(C^2S)_J = 2\left(\sum_K a_{jK} C^K_{j,I} V_K\right)^2,$$

where $C^K_{j,I}$ is the expansion coefficient of the one-quasiparticle Nilsson state in a spherical basis, j is the spin of the state, and the a_{jK} are determined by Coriolis mixing of neighboring single-quasihole states. If Coriolis coupling is neglected the spectroscopic factor reduces to

$$(C^2S)_j = 2(C^K_{j,I})^2 V_K^2 .$$

Coriolis coupling is crucial to understanding the intensity patterns of several strongly coupled bands. To show which bands are strongly coupled, spectroscopic factors calculated without Coriolis coupling are included (in parentheses) in Tables III and IV along with the spectroscopic factors from the full calculation.

V. DISCUSSION

It is difficult to separate the spectroscopic implications of the present investigation from those related to the reaction mechanism. Several aspects of this study are discussed below under headings which indicate whether their greatest relevance is to a spectroscopic or a mechanism

TABLE II. Quantum numbers of bound state orbitals used to calculate form factors for DWBA calculations.

n	l	j
3	s	$\frac{1}{2}$
3	p	$\frac{1}{2}$
3	p	$\frac{3}{2}$
2	d	$\frac{3}{2}$
2	f	$\frac{5}{2}$
2	f	$\frac{7}{2}$
1	g	$\frac{9}{2}$
1	h	$\frac{9}{2}$
1	h	$\frac{11}{2}$
1	i	$\frac{13}{2}$

TABLE III. Excitation energies for ^{163}Dy levels populated through the ^{164}Dy$(d,t)^{163}$Dy reaction. Except for weakly populated states these excitation energies are accurate to ±2 keV. Nilsson model assignments have been taken from Ref. 11, except where otherwise indicated. l values have been derived from angular distribution shapes and, for levels with no previous Nilsson model assignment, spectroscopic factors correspond to the observed l transfer. Several levels whose Nilsson assignment has been reported in previous work show angular distributions characteristic of l values incompatible with that l assignment; in these cases spectroscopic factors are shown for both possible l transfers (see text for discussion).

E_x (MeV)	l	^{163}Dy Nilsson model [a] assignment	S_{exp}	S_{model}		$\frac{d\sigma}{d\Omega}$ ($\theta = 30°$) (μb/sr)
0.000	3	$\frac{5}{2}\frac{5}{2}^-[523]$	0.10	0.070	(0.068)	74
0.074	3	$\frac{7}{2}\frac{5}{2}^-[523]$	0.081	0.11	(0.14)	60
0.167	5	$\frac{9}{2}\frac{5}{2}^-[523]$	0.74	0.83	(0.74)	48
0.248	2	$\frac{5}{2}\frac{5}{2}^+[642]$	0.023	0.005	(0.004)	25
0.283	(4) [b]	$\frac{11}{2}\frac{5}{2}^-[523]$ ($l=4$; 0.095) [c]	0.32	0.037	(0.050)	19
0.335	4	$\frac{9}{2}\frac{5}{2}^+[642]$ [d]	0.66	0.21	(0.17)	170
0.351	1	$\frac{1}{2}\frac{1}{2}^-[521]$	0.072	0.071	(0.071)	210
0.392	1	$\frac{3}{2}\frac{1}{2}^-[521]$ [e]	0.007	0.013	(0.017)	18
0.422	1	$\frac{3}{2}\frac{3}{2}^-[521]$	0.20	0.15	(0.13)	600
0.450	3		0.049			19
0.474	b	$\frac{5}{2}\frac{3}{2}^-[521]$	0.036	0.014	(0.009)	21
0.497	6	$\frac{13}{2}^+$ [f]	1.3	1.8	(1.5)	64
0.514	3	$\frac{7}{2}\frac{1}{2}^-[521]$	0.30	0.22	(0.060)	200
0.552	3	$\frac{7}{2}\frac{3}{2}^-[521]$	0.40	1.0	(0.90)	180
0.591	b	$\frac{9}{2}\frac{1}{2}^-[521]$ [g]	0.20	0.15	(0.067)	12
0.612	1		0.005			25
0.645	5	$\frac{9}{2}\frac{3}{2}^-[521]$	0.32	0.68	(0.61)	15
0.717	b	$\frac{13}{2}\frac{7}{2}^+[633]$	0.32	0.96	(0.24)	15
0.737	0	$\frac{1}{2}\frac{1}{2}^+[660]$	0.14	0.004	(0.004)	230
0.760	h	$\frac{3}{2}\frac{1}{2}^+[660]$	0.025	0.001	(0.001)	30
		$\frac{11}{2}\frac{3}{2}^-[521]$	0.12	0.13	(0.12)	
0.773	(2)	$\frac{5}{2}\frac{1}{2}^+[660]$	0.024	0.046	(0.050)	28
0.792	1		0.060			77
0.806	(1) [b]	$\frac{7}{2}\frac{5}{2}^-[512]$ [e] ($l=1$; 0.012)	0.050	0.010	(0.095)	30
0.825	(1)		0.008			23
0.857	2	$\frac{3}{2}\frac{3}{2}^+[402]$	0.70	1.7	(1.6)	140
0.882	0		0.080			140
0.893	(0)		0.020			33
0.911	b	$\frac{9}{2}\frac{5}{2}^-[512]$	0.87	0.005	(0.026)	60
0.933	2		0.060			45
0.947	3		0.11			62
0.964	0		0.019			34
0.988	(2)		0.048			32
1.050	1		0.16			

TABLE III. *(Continued)*

E_x (MeV)	l	^{163}Dy Nilsson model [a] assignment	S_{exp}	S_{model}		$\frac{d\sigma}{d\Omega}$ ($\theta = 30°$) (μb/sr)
1.059	0	$\frac{1}{2}\frac{1}{2}^+[400]$	0.52	1.2	(1.2)	1020
1.083	2	$\frac{3}{2}\frac{3}{2}^+[651]$	0.14	0.002	(0.001)	86
1.109	0		0.026			40
1.128	2		0.13			78
1.145	0		0.021			29
1.164	b	$\frac{1}{2}\frac{1}{2}^-[510]$ [e]	0.009	0.0004	(0.0002)	21
1.191	(0)		0.007			15
1.198	(2) [b]	$\frac{3}{2}\frac{1}{2}^-[510](l=2; 0.089)$	0.089	0.035	(0.032)	90
1.217	(2)		0.020			9
1.250	(3)		0.04			17
1.276	(3) [b]	$\frac{3}{2}\frac{1}{2}^-[530](l=3; 0.22)$	0.060	0.25	(0.26)	130
1.312	0		0.003			25
1.339	(0)		0.004			6
1.360	(3)	$\frac{7}{2}\frac{1}{2}^-[530]$	0.027	0.26	(0.49)	25
1.395	(1)		0.008			18
1.427	(0) [b]	$\frac{9}{2}\frac{1}{2}^-[530](l=0; 0.003)$	0.77	0.61	(0.82)	24
1.499	(2)		0.034			18
1.527	(1)		0.023			50
1.572	1		0.019			37
1.613	1		0.017			32
1.631	3		0.11			50
1.649	i					7
1.660	(3)		0.046			19
1.691	1		0.025			46
1.708	3		0.22			92
1.753	1		0.057			110
1.812	i					18
1.843	(3) [b]	$\frac{7}{2}\frac{7}{2}^+[404](l=3; 0.33)$	1.8	1.9	(1.9)	130
1.876	(3)		0.17			63
1.949	1		0.030			48
1.986	2		0.044			16
2.042	2		0.064			26
2.105	b					17
2.156	(0)		0.012			14
2.179	b					17
2.194	(1)		0.012			13
2.275	2		0.036			12
2.285	(2)		0.040			32
2.378	3		0.27			80

TABLE III. *(Continued)*

E_x (MeV)	l	^{163}Dy Nilsson model [a] assignment	S_{exp}	S_{model}	$\frac{d\sigma}{d\Omega}$ ($\theta = 30°$) (μb/sr)
2.387	2		0.18		60
2.609	(3)		0.048		10
2.645	(1)		0.082		15
2.691	b				12

[a] As is discussed in the text, there is evidence for large vibrationally-coupled components in the wave functions of several of these states. The only component listed here for each state is the single-quasihole component (the only component which should be involved in a one-step reaction).

[b] Anomalous angular distribution shape (see Fig. 6).

[c] Funke *et al.* (Ref. 14) report evidence for a $\frac{7}{2}^+$ state at 0.286 MeV in ^{163}Dy which they assign to be $\frac{7}{2}\frac{7}{2}^+$[633].

[d] Reference 10.

[e] Differs by more than 2 keV from the excitation energy reported in Ref. 11 so the identification of the state is less certain.

[f] Reference 15. The model spectroscopic factor has been calculated assuming an assignment $\frac{13}{2}\frac{5}{2}^+$[642].

[g] Assignment of this state as $\frac{9}{2}\frac{1}{2}^-$[521] fits in quite well with the excitation energy prediction of the calculation described in the text. However, the transition shows an angular distribution which cannot be identified with any l value.

[h] Doublet can be plausibly fitted with an incoherent mixture of $l = 2$ and $l = 5$ angular distributions with spectroscopic strengths as indicated above.

[i] Clearly observed in five or more spectra, but populated weakly and/or obscured by impurities or stronger transitions in enough spectra that no meaningful angular distribution could be extracted.

question, but before proceeding with this arbitrary classification the following general cautions should be noted:

(1) Implications drawn from angular distribution shapes are proposed with far more confidence then are implications drawn from spectroscopic factors (dis)agreements. The Nilsson model predictions of spectroscopic factors are, in many cases, quite sensitive to the assumed Coriolis coupling strength. As is mentioned above, the observed energy spectra are not well reproduced unless these Coriolis matrix elements are reduced to ~ 60% of their values in the pure Nilsson model. This prescription has evolved from results of many experiments[31] and has received further support from the attempts of Damgaard, Kusuno, and Faessler[32] to explain backbending of yrast bands. This 60% reduction of the Coriolis coupling seems currently the most reasonable procedure, and there are equally great or greater discrepancies between the experimental spectroscopic factors and those resulting from Nilsson model calculations either without Coriolis coupling (shown in parentheses in Tables III and IV) or with full Coriolis coupling. However, this sensitivity of the model spectroscopic factors to the assumed strength of the Coriolis coupling adds another source of uncertainty to interpreting the spectroscopic factor discrepancies discussed below. The model-predicted spectroscopic factors are even less reliable for the (positive parity) bands which are subject to $\Delta N = 2$ mixing. I.e., two downward sloping (with increasing deformation) $N = 6$ orbitals, $\frac{1}{2}^+$[660] and $\frac{3}{2}^+$[651], encounter two upward sloping $N = 4$ orbitals, $\frac{1}{2}^+$[400] and $\frac{3}{2}^+$[402], just below the $N = 97$ Fermi surface.[33] The interactions between pairs of levels based on orbitals such as these have been studied[34] but are not at all well established. In addition to these features which complicate the calculation of Nilsson model spectroscopic factors, the DWBA analysis of the experiment is much less straightforward than it would be for a (d,t) reaction on a closed shell nucleus. As is discussed above, the form factors used in the DWBA analysis were calculated with spherical Woods-Saxon binding wells whose depths was adjusted according to the binding energy prescription (with no configuration mixing). Such a procedure is only justifiable for a single particle outside a closed shell; normalizing such a wave function almost certainly introduces distortions in the form factor at the surface of a deformed

TABLE IV. Excitation energies for ^{165}Er levels populated through the ^{166}Er$(d,t)^{165}$Er reaction. Except for weakly populated states, these excitation energies are accurate to ±2 keV. Nilsson model assignments have been taken from Ref. 12, except where otherwise indicated. l values have been derived from angular distribution shapes and, for levels with no previous Nilsson model assignment, spectroscopic factors correspond to the observed l transfer. Several levels whose Nilsson assignment has been reported in previous work, show angular distributions characteristic of l values incompatible with the previous assignment; in these cases spectroscopic factors are shown for both possible l transfers (see text for discussion).

E_x (MeV)	l	^{165}Er Nilsson model assignment	S_{exp}	S_{model}		$\frac{d\sigma}{d\Omega}$ ($\theta = 30°$) (μb/sr)
0.000	3	$\frac{5}{2}\frac{5}{2}^-[523]$	0.090	0.071	(0.068)	50
0.051	a	$\frac{5}{2}\frac{5}{2}^+[642]$	0.039	0.003	(0.003)	33
0.076	3	$\frac{7}{2}\frac{5}{2}^-[523]$	0.060	0.084	(0.14)	32
0.097	4	$\frac{9}{2}\frac{5}{2}^+[642]$	0.92	0.13	(0.13)	110
0.174	5	$\frac{9}{2}\frac{5}{2}^-[523]$	1.0	0.91	(0.74)	35
0.241	1	$\frac{3}{2}\frac{3}{2}^-[521]$	0.17	0.13	(0.11)	360
0.296	1	$\frac{1}{2}\frac{1}{2}^-[521]$	0.11	0.096	(0.096)	240
0.356	1	$\frac{3}{2}\frac{1}{2}^-[521]$	0.020	0.027	(0.023)	40
0.371	3	$\frac{7}{2}\frac{3}{2}^-[521]$	0.71	1.2	(0.80)	280
0.383	a	$\frac{5}{2}\frac{1}{2}^-[521]$	0.11	0.072	(0.069)	45
0.431	0		0.021			30
0.467	a	$\frac{9}{2}\frac{3}{2}^-[521]$	0.40	0.69	(0.55)	15
0.505	0	$\frac{1}{2}\frac{1}{2}^+[660]$ [b]	0.17	0.004	(0.004)	400
0.532	2	$\frac{3}{2}\frac{3}{2}^+[402]$	0.57	1.6	(1.5)	390
0.547	a	$\frac{11}{2}\frac{11}{2}^-[505]$ [c]	1.7	1.8	(1.8)	63
0.573	(3)	$\frac{7}{2}\frac{5}{2}^-[512]$	0.10	0.005	(0.18)	40
0.587	d	$\frac{3}{2}^+ + (\frac{1}{2},\frac{3}{2})^-[0.03(l=1)+0.02(l=2)]$				70
0.599	(2)		0.071			35
0.648	e					15
0.674	2		0.021			12
0.721	e					15
0.741	0	$\frac{1}{2}\frac{1}{2}^+[400]$ [b]	0.28	1.1	(1.1)	420
0.760	3		0.24			82
0.817	3 [a]	$\frac{11}{2}\frac{5}{2}^-[512]$ [f] $(l=3; 0.34)$	1.7	0.013	(0.010)	150
0.840	(1)		0.008			10
0.863	2		0.084			36
0.920	(1)	$\frac{1}{2}\frac{1}{2}^-[510]$	0.006	0.0008	(0.0004)	10
0.955	(4)		0.3			30
0.971	(2)		0.02			10
1.039	1	$\frac{3}{2}\frac{1}{2}^-[530]$	0.20	0.24	(0.26)	300
1.064	(1) [a]	$\frac{5}{2}\frac{1}{2}^-[530](l=1; 0.026)$	0.073	0.16	(0.18)	35
1.106	(3)		0.069			13
1.139	2		0.074			25
1.172	(3)	$\frac{7}{2}\frac{1}{2}^-[530]$ [g]	0.10	0.31	(0.48)	35

TABLE IV. *(Continued)*

E_x (MeV)	l	^{165}Er Nilsson model assignment	S_{exp}	S_{model}	$\frac{d\sigma}{d\Omega}$ ($\theta = 30°$) (μb/sr)
1.250	c				10
1.274	(3)		0.26		80
1.290	(1)		0.02		30
1.332	c				20
1.379	(3)		0.10		36
1.411	c				10
1.489	0		0.11		92

[a] Anomalous angular distribution shape (see Fig. 10).

[b] As is discussed in the text, there is much evidence for especially strong $\Delta N = 2$ and Coriolis distortion of the positive parity bands; the labeling above simply follows that of Ref. 12 for convenience.

[c] See Refs. 19 and 21.

[d] This is reported to be a doublet by Kurcewicz *et al.* (Ref. 16) and its angular distribution can plausibly be fitted with the indicated mixture of $l = 1$ and $l = 2$ strengths (see Fig. 10). The previous assignment of this group was $\frac{11}{2}\frac{11}{2}^-[505]$.

[e] Angular distribution poorly fitted with any l value, but the level is only very weakly populated.

[f] This assignment from Ref. 12 has been questioned; see discussion in Ref. 6, Table IV.13, footnote i.

[g] Reference 15 suggests that this level was misidentified in Ref. 12 and that this transition should be $l = 5$ or 6. The present data (see Fig. 8) are not well reproduced with any l value but $l = 3$ gives the best agreement.

nuclide of the sort considered here. Rost has calculated couplings between channels in the expansion of a deformed single-particle wave function and has found sizable changes in normalization of individual form factors at the nuclear surface.[35] Unfortunately, the appplication of Rost's procedure is not only difficult, but also involves an interplay between the assumed details of the structure of each nuclear state and the reaction mechanism assumptions. As was stated above, the conventional DWBA is used to organize the experimental results of this investigation and further model-dependent adjustments of the form factors used in the analysis would be inappropriate.

(2) While it is assumed below that the orbital angular momentum transfer l of a transition is well determined if the measured angular distribution is well fitted by the DWBA prediction for some l, this is not necessarily the case. Figures 6 and 10 provide ample evidence that at least some transitions are not susceptible to DWBA analysis. It is conceivable that interference patterns in angular distributions which result from multistep processes could look like DWBA patterns for the wrong l value. Ascuitto *et al.* have reported oscillatory structure in angular distributions which, on the basis of CCBA calculations, they have attributed to multistep effects.[1] Some of the effects seen by Ascuitto *et al.* are sufficiently small that such angular distributions are not classified as anomalous in this work where it has not been possible to perform CCBA calculations.

A. Spectroscopic information from angular distribution shapes

The anomalous angular distributions [those whose shape is not well fitted at all or at least not by DWBA calculations which use an l value consistent with the previously assigned angular momentum parity (J^π) of the state] are grouped in Figs. 6 and 10. While the angular distributions on the left sides of Figs. 6 and 10 cannot be fitted with DWBA calculations for any l value, those on the right can be fitted on the assumption that the previous work misidentified the state.

In ^{163}Dy these latter states are: 0.283 MeV (previously assigned $\frac{11}{2}$ member of the $\frac{5}{2}^-[523]$ band; currently fitted with $l = 4$); 0.806 MeV (previously a level at 0.801 MeV was assigned $\frac{7}{2}$ member of the $\frac{5}{2}^-[512]$ band; currently fitted with $l = 1$); 1.198 MeV (previously assigned $\frac{3}{2}$ member of the $\frac{1}{2}^-[510]$ band; presently fitted with $l = 2$); 1.276 MeV (previously assigned $\frac{3}{2}$ member of the $\frac{1}{2}^-[530]$ band;

TABLE V. Bandhead energy, moment of inertia parameters, decoupling parameters, and level fullness parameters V^2 from fitting the energy spectra of ^{163}Dy and ^{165}Er as described in the text.

Nuclide	Nilsson band	Bandhead energy (keV)	Moment of inertia	Decoupling parameter	V^2
^{163}Dy	$\frac{5}{2}^-[523]$	0	10.6		0.50
	$\frac{1}{2}^-[521]$	351	10.7	0.265	0.14
	$\frac{3}{2}^-[521]$	422	11.8		0.89
	$\frac{5}{2}^-[512]$	715 [a]	11.2		0.063
	$\frac{1}{2}^-[530]$	1255 [a]	b		0.97
	$\frac{1}{2}^-[510]$	1164	13.3	0.03	0.038
	$\frac{5}{2}^+[642]$	251	9.3		0.83
	$\frac{7}{2}^+[633]$	a	b		0.90
	$\frac{1}{2}^+[660]$	737 [c]	6.2	0.49 [c]	0.13
	$\frac{3}{2}^+[402]$	857 [c]	10.7		0.95
	$\frac{1}{2}^+[400]$	1059 [c]	b, c	c	0.96
	$\frac{3}{2}^+[651]$	1083 [c]	b, c		0.96
	$\frac{7}{2}^+[404]$	1843	b		0.98
^{165}Er	$\frac{5}{2}^-[523]$	0	11.1		0.50
	$\frac{3}{2}^-[521]$	242	12.3		0.79
	$\frac{1}{2}^-[521]$	296	12.2	0.522	0.19
	$\frac{5}{2}^-[512]$	481 [a]	10.4		0.12
	$\frac{11}{2}^-[505]$	547	b		0.92
	$\frac{1}{2}^-[510]$	920	13.1	0.04	0.07
	$\frac{1}{2}^-[530]$	992 [a]	10.1		0.94
	$\frac{5}{2}^+[642]$	51	2.9		0.63
	$\frac{1}{2}^+[660]$	505 [c]	b	c	0.88
	$\frac{3}{2}^+[402]$	532 [c]	b		0.88
	$\frac{1}{2}^+[400]$	741 [c]	b	0.131 [c]	0.91

[a] Bandhead not observed. Where a number is indicated, this number was assumed for calculational purposes.

[b] Not well determined because too few members of the band were observed.

[c] Strong $\Delta N = 2$ mixing makes these parameters very uncertain.

presently fitted with $l = 3$); 1.427 MeV (previously assigned $\frac{9}{2}$ member of the $\frac{1}{2}^-[530]$ band; presently fitted with $l = 0$); and 1.843 MeV (previously assigned $\frac{7}{2}$ member of the $\frac{7}{2}^+[404]$ band; presently fitted with $l = 3$). Not only does the previous assignment of the 0.283 MeV fit well with the expected excitation energy pattern of the ground state rotational band but it also agrees with the Coulomb excitation work of Tveter and Herskind[13] who observe a fast γ decay of this state as if it were a member of the ground state band. Earlier γ decay work by Funke *et al.*[14] tentatively placed the $\frac{7}{2}$ member of the $\frac{7}{2}^+[633]$ band at 0.286 MeV which might indicate a doublet structure where the $l = 4$ component dominates in the (d,t) reaction. However, this $l = 4$ transition is expected to have a very small spectroscopic factor (less than 0.001 with the Coriolis coupling discussed above and smaller without Coriolis coupling) so the transition may well result from multistep processes. The 0.806 MeV level is weakly populated so its excitation energy is uncertain. It may not be the same level as is strongly populated with the (d,p) reaction.[11]

The 1.198, 1.276, 1.427, and 1.843 MeV levels were previously assigned entirely on the basis of (d,t) spectra measured with 12 MeV deuterons[11] and so these assignments must almost certainly

be dropped. It is interesting that the present $l = 3$ assignment contradicts the $\frac{7}{2}^+[404]$ assignment of the 1.843 MeV state since the previously assigned $\frac{7}{2}^+[404]$ bandheads in ^{159}Gd and ^{161}Dy also failed to show $l = 4$ patterns when (d,t) angular distributions became available.[9]

The 0.497 MeV state in ^{163}Dy had been assigned $\frac{11}{2}\ \frac{11}{2}^-[505]$ from 12 MeV (d,t) spectra[11] but Grotdal *et al.* reassigned this state to have spin-parity $\frac{13}{2}^+$ on the basis of its excitation in $(^3\text{He},\alpha)$ spectra.[15] As is discussed in Ref. 8, rather well fitted (d,t) angular distributions populating states of known spin-parity in this and other rare-earth nuclei tend systematically to show small angle cross sections which are slightly larger than that predicted by the DWBA for the correct l value and slightly smaller than the DWBA prediction for the next smaller l value. On this basis the angular distribution for (d,t) population of the 0.497 MeV (shown in Fig. 5) is more reasonably fitted by $l = 6$ than by $l = 5$ and so is consistent with the assignment of Grotdal *et al.*[15] Grotdal *et al.* place the bandhead of the $\frac{11}{2}^-[505]$ band at 0.849 MeV.[15] The strong $l = 2$ transition to the state at 0.857 MeV makes it unrealistic to expect to see even a strong $l = 5$ transition to such a nearby level, and indeed no evidence for a 0.849 MeV state is observed in this study.

Table III shows 11 $l = 0$ transitions to states below $E_x = 1.5$ MeV in ^{163}Dy. This indicates that the strength available in at least one of the two available $l = 0$ single-particle states ($\frac{1}{2}^+[400]$ and $\frac{1}{2}^+[660]$) is fragmented through mixing with very many other states. Neglected interactions between single-particle states (e.g., $\Delta N = 2$ mixing) cannot be expected to produce such extra s states; this fragmentation probably indicates considerable mixing with vibration-coupled configurations. It is interesting that ^{164}Dy(d,t) ^{163}Dy shows approximately twice as many $l = 0$ transitions to the low excitation energy region as do any of the other reactions studied in this series of experiments. [Table IV shows that the ^{166}Er$(d,t)^{165}$Er reaction yields four $l = 0$ transitions to states below $E_x = 1.5$ MeV.]

There are two levels in ^{165}Er whose angular distributions are well fitted by assuming an l value incompatible with their previous Nilsson model assignment: The 0.817 MeV state was assigned[12] as the $\frac{11}{2}$ member of the $\frac{5}{2}^-[512]$ band but is fitted best as $l = 3$; and the 1.064 MeV state was previously assigned[12] to be the $\frac{5}{2}$ member of the $\frac{1}{2}^-[530]$ band, but it is best fitted as $l = 1$. Along with these two angular distributions, the right side of Fig. 10 also contains the angular distribution for the transition to the group at 0.587 MeV. This had been assigned as the $\frac{11}{2}$ member of the $\frac{11}{2}^-[505]$ band on the basis of 12 MeV (d,t) spectra,[12] but both $(^3\text{He},\alpha)$ spectra[21] and an $(\alpha, xn\gamma)$ investigation[19] place the $\frac{11}{2}^-[505]$ bandhead at 0.547 MeV. Kurcewicz *et al.*[16] have observed ^{165}Er γ decays which follow electron capture by ^{165}Tm and report that the level at 0.587 MeV is a doublet of states, with spin-parities $\frac{3}{2}^+$ and $(\frac{1}{2}, \frac{3}{2})^-$. As can be seen from the right side of Fig. 10 the angular distribution for this transition can be fitted plausibly with a combination of $l = 1$ and $l = 2$ strength.

Lovhoiden, Tjom, and Edvardson[21] have measured ^{166}Er$(^3\text{He},\alpha)$ spectra to search for high l strength. In addition to the evidence noted above for the position of the $\frac{11}{2}^-[505]$ bandhead, they report a $\frac{13}{2}^+$ state at 0.238 MeV and suggest that the 1.172 MeV state (assigned $\frac{7}{2}\ \frac{1}{2}^-[530]$ by Tjom and Elbek[12]) should be $l = 5$ or $l = 6$. No 0.238 MeV state is seen in this work, nor should one be seen since such a high l transition would be masked by the strong $l = 1$ transition to the $\frac{3}{2}\ \frac{3}{2}^-[521]$ state at 0.241 MeV. The transition to the 1.172 MeV level seen in this work shows an $l = 3$ angular distribution, consistent with the original assumption of Tjom and Elbek.[12]

B. Reaction mechanism information from angular distribution shapes

The angular distributions shown on the left sides of Figs. 6 and 10 provide strong evidence for a breakdown of one or more of the one-step direct reaction assumptions involved in performing a DWBA analysis. None of these angular distributions has been fitted with any DWBA calculation. Obviously some of these transitions, particularly at high excitation energy, could populate unresolved doublets, but most of them populate levels whose Nilsson model assignment has been rather confidently established and so are almost certainly transitions to individual well-resolved states whose angular distributions are anomalous. In ^{165}Er the 0.051 MeV state (Fig. 10) is well known[12,16,18,19] to have $J^\pi = \frac{5}{2}^+$. The J^π and Nilsson band assignments have also been well established for the 0.383 $(\frac{5}{2}^-)$[13,16,20] and 0.547 $(\frac{11}{2}^-)$[18,19,21] MeV states of ^{165}Er. ^{163}Dy has been less extensively studied but particularly the assignment of the 0.474 MeV[10,11,13,14] state seems convincing; most important, none of the available evidence indicates a doublet structure for any of the levels listed as anomalous for either nucleus.

As was reported in Ref. 8 there are several Nilsson bands of which at least one member exhibits an anomalous angular distribution in at least four of the five residual nuclides ^{159}Gd, ^{161,163}Dy, and ^{165,167}Er. These bands are: $\frac{11}{2}^-[505]$, $\frac{1}{2}^-[521]$, and $\frac{3}{2}^-[521]$. The $\frac{1}{2}^-[521]$ and $\frac{3}{2}^-[521]$ bands also tend to exhibit somewhat greater discrepancies

between experimental and model spectroscopic factors than do members of other bands, but this effect is difficult to assess in view of the spectroscopic factor uncertainties discussed above.

As was discussed above, the transition to the $\frac{11}{2}^-[505]$ bandhead in ^{163}Dy cannot be observed with the (d,t) reaction because of a strong nearby $l=2$ transition, but this level is observed in ^{165}Er where the angular distribution is anomalous (as it is[8,9] in ^{159}Gd, ^{161}Dy, and ^{167}Er). All the observed transitions to $\frac{11}{2}^-[505]$ single-hole states have shown angular distributions which are distinctly different from those of other $l=5$ transitions observed in this mass region.

In ^{163}Dy the $\frac{9}{2}$ member of the $\frac{1}{2}^-[521]$ band shows an anomalous angular distribution while in ^{165}Er the $\frac{5}{2}$ member of this band shows an anomaly. In each of these nuclei there is considerable evidence of strong mixing of the $\frac{1}{2}^-[521]$ single-hole configuration with vibrationally-coupled terms of the form $\{\frac{5}{2}^-[523], 2^+\}$.[6,13,36] This, coupled with the presence of anomalous (d,t) angular distributions to members of this band in four neighboring nuclei, clearly suggests a multistep reaction mechanism. On the other hand, members of the $\frac{3}{2}^-[521]$ band show anomalous angular distributions

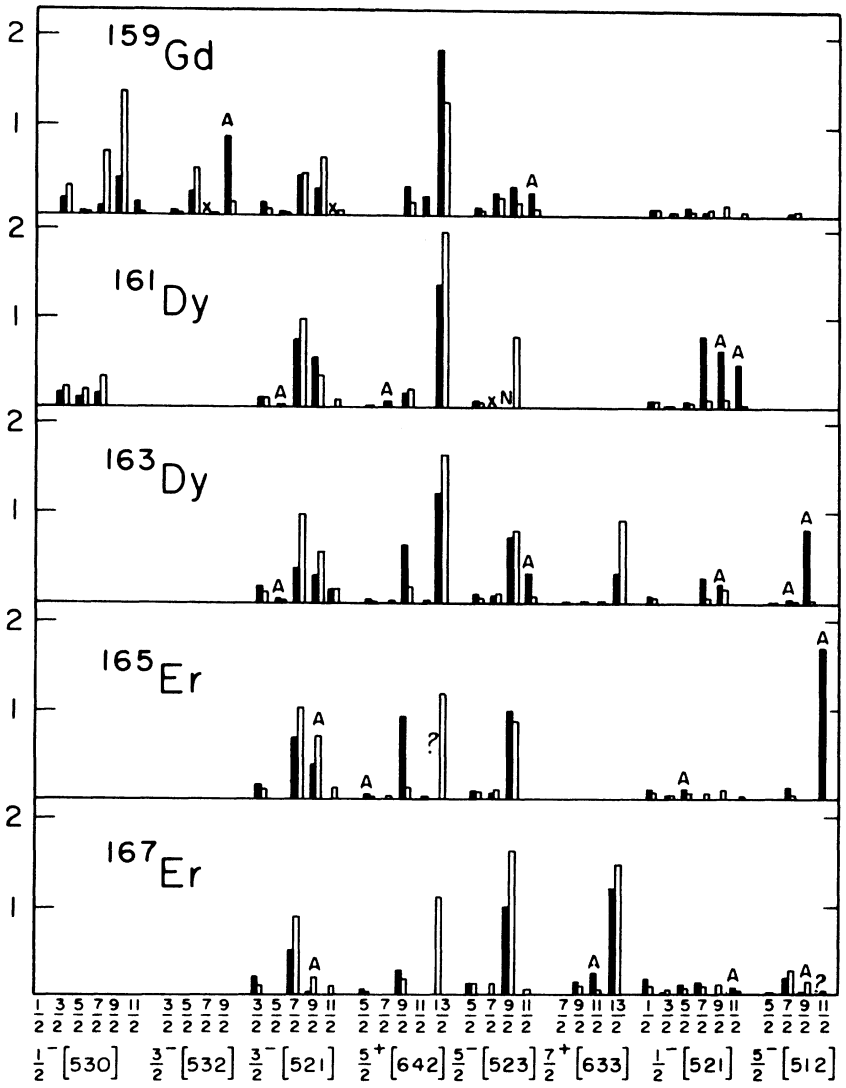

FIG. 11. The solid bars represent experimental spectroscopic factors for the (d,t) population of the indicated states. The open bars represent spectroscopic factors predicted by the Nilsson model calculation described in the text. The excitation energy of the Nilsson model single-particle states increases from left to right along the abscissa so the Fermi level shifts to the right as the neutron number increases from 95 at the top of the figure to 99 at the bottom. The four positive parity bands which are most subject to strong ΔN mixing are not included in the figure (see text for discussion).

in the same four neighboring nuclei and there is no evidence from electromagnetic transition studies of any strong mixing of this band with vibrationally-coupled configurations.

As was noted above, several of the easily identified anomalous angular distributions shown in Figs. 6 and 10 are high l cases which have large cross sections at small angle. Attributing this filling in of the expected small angle minimum to multistep processes seems reasonable because most inelastic transitions that could contribute to the population of these high spin levels by multistep routes would tend to reduce the l which is transferred with the neutron and these l reductions could plausibly fill in the forward angle cross section.

It is obviously of interest to try to understand why some transitions exhibit angular distribution patterns that agree well with DWBA predictions while others deviate so markedly as those discussed above. Cotanch and Vincent[37] have recently developed a method to approximate CCBA calculations which not only require less computer time than does a full CCBA calculation but which also may allow greater insight into the sensitive features of the calculation. Hopefully the results of the present investigation will provide a suitable data base for an investigation with such calculations of the structure and/or dynamical conditions under which the one-step DWBA assumptions break down.

C. Information from spectroscopic factors

Figure 11 compares the measured spectroscopic factors with those predicted by the Nilsson model for members of several rotational bands. Figure 11 includes spectroscopic factors extracted from (d, t) measurements on five rare earth targets. The information on ^{159}Gd and ^{161}Dy has been reported in detail in Ref. 9; except for a preliminary report[38] and a small part of the data which was included in Ref. 8, the ^{167}Er data are, as yet, unpublished. However, it seems worthwhile to include all these systems in Fig. 11 to provide a perspective for assessing the value of the spectroscopic factors presented here. The Nilsson bands in Fig. 11 are arranged in order of increasing energy and it is possible to follow the shift of the Fermi energy to the right of the figure as neutron number increases from 95 (^{159}Gd and ^{161}Dy) to 99 (^{167}Er). Spectroscopic factors marked with an A in Fig. 11 correspond to transitions which exhibited anomalous angular distributions. These result from fitting the DWBA cross sections to the average level of the poorly fit experimental angular distributions and are inherently more uncertain than the other spectroscopic factors shown in the figure. Results for members of four positive parity bands ($\frac{1}{2}^+[400]$, $\frac{1}{2}^+[660]$, $\frac{3}{2}^+[402]$, and $\frac{3}{2}^+[651]$) are not included in Fig. 11 because these bands are well known[33] to show signs of strong $\Delta N = 2$ mixing (see discussion above) and are not well fitted in any of five residual nuclides. Spectroscopic factors for members of these bands are, however, included in Tables III and IV. While Fig. 11 and Tables III and IV show that many transitions are observed to agree in absolute cross section with Nilsson model predictions, there are obviously many disagreements as well. The above-mentioned difficulties with $\Delta N = 2$ mixing, Coriolis coupling, and form factor normalizations certainly restrict the conclusions which can be drawn from comparing the experimental spectroscopic factors with those predicted by the Nilsson model calculation. However, the Coriolis coupling prescription employed herein is probably reasonable and Rost's estimate[35] indicates that the form factor normalization problems only introduce ~30% extra uncertainty in the more troublesome cases. So most of the spectroscopic factors for the negative parity levels shown in Fig. 11 and Tables III and IV should probably agree within $\lesssim$50% with the Nilsson model expectations. Many of these spectroscopic factors disagree with the model by a factor of 2 or more, and either this indicates unexpectedly strong vibration-quasiparticle mixing,[36] or it may indicate that many of these transitions do not proceed as pure one-step direct transfers.

Spectroscopic factor sums for each l value are listed in Table VI. These have been compiled on

TABLE VI. Summed spectroscopic strengths for all observed l values. States identified in Tables III and IV with a rotational band built on a specified Nilsson level are assumed to have been correctly identified. Strengths of transitions to previously unidentified states whose angular distributions show characteristic l patterns have also been included. The model predictions include only the levels identified in Tables III and IV and since more Nilsson states have been identified in ^{163}Dy than in ^{166}Er, the model sum limits are different.

	^{163}Dy		^{165}Er	
l	Exp.	Model	Exp.	Model
0	0.86	1.2	0.58	1.1
1	0.79	0.52	0.56	0.50
2	1.6	1.7	0.90	1.6
3	2.0	1.7	1.9	1.9
4	2.5	2.1	1.2	0.13
5	3.3	2.4	4.8	3.4
6	1.6	2.8	0	0
Total	12.7	11.4	9.9	8.6

the assumption that all Nilsson model assignments listed in Tables III and IV—including those levels discussed above as showing anomalous or incompatible l angular distributions—have been correctly identified. These spectroscopic factor sums agree well with the model calculations. Even though the ^{165}Er spectrum is more compressed than that of ^{163}Dy, more Nilsson bands are identifiable in ^{163}Dy and so the model calculation for ^{163}Dy allows a larger summed limit, ~11.

Considerable pickup strength may well be spread over many vibrationally-coupled states—indeed, both Tables III and IV show a significant number of transitions which are not identified as to Nilsson model configuration, but which contribute to the experimental spectroscopic sums in Table VI. This complements the other indications of fragmentation of single-particle strength discussed above.

Overall the spectroscopic factor sums are in surprisingly good agreement with Nilsson model expectations. This was also the case for the 12 MeV (d, t) work (on these and neighboring rare-earth nuclei)[5] where this agreement, combined with the lack of complete angular distributions, seemed to indicate that the DWBA assumptions and the Nilsson model meshed well to account for the data. Several of the few available 12 MeV angular distributions [on ^{160}Gd$(d, t)^{159}$Gd] did show deviations from DWBA-predicted shapes[39]; an attempt was made to construct an approximate correction to the DWBA for multistep effects[40]; and the Nilsson band "signatures" for the individual spectra of the nuclei in this mass region[5] did show several large discrepancies of the sort shown in Fig. 11. But the surprising overall spectroscopic factor agreement (which arises partly from approximate equality of DWBA-predicted peak cross sections and average cross sections for transitions whose angular distributions frequently bear little or no resemblance to DWBA expectations) has tended to foster a confidence in the simplest DWBA + Nilsson model analysis that many of the considerations discussed above would not support.

VI. SUMMARY AND CONCLUSIONS

The shapes of the angular distributions for the (d, t) population of states in ^{163}Dy and ^{165}Er are generally well fitted by DWBA calculations, but a significant number of angular distributions either cannot be fitted with any DWBA calculation or can only be fitted with a DWBA calculation which assumes a different l transfer then would be required if the previously assigned angular momentum parity of the residual state were correct. Departure from a simple one-step direct reaction mechanism is particularly suggested by anomalies which appear in transitions to members of the $\frac{1}{2}^-[521]$ and $\frac{3}{2}^-[521]$ bands in both nuclei and to the $\frac{11}{2}^-[505]$ bandhead in ^{165}Er. Single-quasihole strength appears to be fragmented in several cases; this is especially true of $l = 0$ strength in ^{163}Dy. Such fragmentation may indicate mixing with vibrationally-coupled configurations so that, for high l transitions, multistep processes can be expected to compete with the intrinsically weak one-step direct transfers. Since Cotanch and Vincent[37] have recently developed a method to approximate CCBA calculations (in a format which may allow one to test for the sensitive features of the calculation without using excessively large amounts of computer time), it is hoped that the results of this investigation will provide a suitable data base for an investigation of the structure and/or dynamical conditions under which the one-step DWBA assumptions are applicable.

No evidence is found to indicate the position of the $\frac{7}{2}^+[404]$ single-quasihole state in either ^{163}Dy or ^{165}Er. (The transition to the state at 1.843 MeV in ^{163}Dy—which had previously been associated with this configuration[11]—shows an $l = 3$ angular distribution.)

The spectroscopic factors extracted from the DWBA analysis of the presently reported angular distributions are not in very good agreement with Nilsson model predictions, even for the levels whose angular distributions are rather well fitted. These factor of ~2 discrepancies cannot be entirely ascribed to multistep transfer processes because of uncertainties in the treatment of the deformed form factor in the DWBA analysis of the data and sensitivity of the model-predicted spectroscopic factors to uncertainties in assumed Coriolis coupling strengths and $\Delta N = 2$ wave function admixtures.

ACKNOWLEDGMENTS

We appreciate the help of Dr. J. R. Erskine in providing the code BANDFIT and allowing us to use the Argonne automatic plate scanner. We also acknowledge Dr. C. M. Vincent for several helpful discussions.

*Work supported by the National Science Foundation.

[1]R. J. Ascuitto, C. H. King, and L. J. McVay, Phys. Rev. Lett. 29, 1106 (1972).
[2]R. J. Ascuitto and N. K. Glendenning, Phys. Rev. 181, 1396 (1969); N. K. Glendenning and R. S. Macintosh, Nucl. Phys. A168, 575 (1971).
[3]A. K. Abdallah, T. Udagawa, and T. Tamura, Phys. Rev. C 8, 1855 (1973); D. K. Olsen, T. Udagawa, T. Tamura, and R. E. Brown, *ibid.* 8, 609 (1973).
[4]N. Austern, *Direct Nuclear Reaction Theories* (Wiley-Interscience, New York, 1970), and references therein; S. K. Penny and G. R. Satchler, Nucl. Phys. 53, 145 (1964).
[5]B. Elbek and P. J. Tjom, in *Advances in Nuclear Physics,* edited by M. Baranger and E. Vogt (Plenum, New York, 1969), Vol. III, and references therein.
[6]M. E. Bunker and C. W. Reich, Rev. Mod. Phys. 43, 348 (1971).
[7]J. J. Kolata and J. V. Maher, Phys. Rev. C 8, 285 (1973).
[8]J. V. Maher, G. H. Wedberg, J. J. Kolata, J. C. Peng, and J. L. Ricci, Phys. Rev. C 8, 2390 (1973).
[9]J. C. Peng, J. V. Maher, G. H. Wedberg, and C. M. Cheng, Phys. Rev. C 3, 1451 (1976).
[10]O. W. B. Schult, M. E. Bunker, D. W. Hafemeister, E. B. Shera, E. T. Jurney, J. W. Starner, A. Bocklin, B. Fogelberg, U. Gruber, B. P. K. Maier, H. R. Kock, W. N. Shelton, M. Minor, and R. K. Sheline, Phys. Rev. 154, 1146 (1967).
[11]T. Grotdal, K. Nybø and B. Elbek, K. Dan. Vidensk. Selsk., Mat.–Fys. Medd. 37, No. 12 (1970).
[12]P. O. Tjøm and B. Elbek, K. Dan. Vidensk. Selsk., Mat.–Fys. Medd. 37, No. 7 (1969).
[13]A. Tveter and B. Herskind, Nucl. Phys. A134, 599 (1969).
[14]L. Funke, H. Graber, K.-H. Kaun, H. Sodan, G. Geske, and J. Frana, Nucl. Phys. 84, 424 (1966).
[15]T. Grotdal, K. Nybø, O. Straume, and T. Thorsteinsen, Phys. Norv. 8, 23, 33 (1975).
[16]W. Kurcewicz, Z. Moroz, Z. Preibisz, and B. Schmidt Nielsen, Nucl. Phys. A108, 434 (1968).
[17]G. T. Adylov, R. Babodzhanov, A. S. Kuchma, and V. A. Morozov, Yad. Fiz. 8, 417 (1968) [Sov. J. Nucl. Phys. 8, 241 (1968)].
[18]B. Hormatz, T. H. Handley, and J. W. Mihelich, Phys. Rev. 128, 1186 (1962); W. Andrejtscheff, P. Manfrass, H. Prade, K. D. Schilling, G. Winter, H. Fuir, R. Ion-Mihai, A. B. Khalikulov, V. A. Morozov, N. Z. Marupov, and T. M. Muminov, Nucl. Phys. A220, 438 (1974).
[19]S. A. Hjorth, H. Ryde, K. A. Hagemann, G. Lovhoiden, and J. C. Waddington, Nucl. Phys. A144, 513 (1970).
[20]N. A. Bouch-Osmolovskaya, K. Ya. Gromov, and W. C. Chu, Nucl. Phys. 81, 225 (1966).
[21]G. Lovhoiden, P. O. Tjøm, and L. O. Edvardson, Nucl. Phys. A194, 463 (1972).
[22]J. R. Erskine and R. H. Vonderohe, Nucl. Instrum. Methods 181, 221 (1970).
[23]J. R. Comfort, ANL Physics Division Informal Report No. PHY-1970B, 1970 (unpublished); P. Spink and J. R. Erskine, ANL Physics Division Informal Report No. PHY-1965B (unpublished).
[24]P. D. Kunz, Univ. of Colorado (unpublished).
[25]E. R. Flynn, D. D. Armstrong, J. G. Beery, and A. G. Blair, Phys. Rev. 182, 1113 (1969).
[26]C. M. Perey and F. G. Perey, Phys. Rev. 132, 755 (1963).
[27]W. W. Daehnick and R. M. DelVecchio, Phys. Rev. C 11, 623 (1975).
[28]W. T. Pinkston and G. R. Satchler, Nucl. Phys. 72, 641 (1965); R. J. Philpott, W. T. Pinkston, and G. R. Satchler, *ibid.* A125, 176 (1969), and references contained therein.
[29]S. G. Nilsson, K. Dan. Vidensk. Selsk., Mat.–Fys. Medd. 29, No. 16 (1955).
[30]J. R. Erskine, Argonne National Laboratory (unpublished).
[31]R. F. Casten, P. Kleinheinz, P. J. Daly, and B. Elbek, Phys. Rev. C 3, 1271 (1971); K. Dan. Vidensk. Selsk., Mat.–Fys. Medd. 38, No. 13 (1972), and references therein.
[32]J. Damgaard, S. Kusuno, and A. Faessler, Nucl. Phys. A243, 492 (1975).
[33]R. K. Sheline, M. J. Bennett, J. W. Dawson, and Y. Shida, Phys. Lett. 26B, 14 (1968); I. Kanestrom, P. O. Tjøm, and J. Bang, Nucl. Phys. A164, 664 (1971).
[34]B. L. Anderson, Nucl. Phys. A196, 547 (1972), and references therein.
[35]E. Rost, Phys. Rev. 154, 994 (1967).
[36]V. G. Soloviev and P. Vogel, Nucl. Phys. A92, 449 (1967), and references therein.
[37]S. R. Cotanch and C. M. Vincent, Phys. Rev. Lett. 36, 21 (1976).
[38]J. L. Ricci, J. J. Kolata, R. Miller, and J. V. Maher, Bull. Am. Phys. Soc. 17, 558 (1972).
[39]M. Jaskola, K. Nybø, P. O. Tjøm, and B. Elbek, Nucl. Phys. A96, 52 (1967).
[40]M. Jaskola and M. Kozlowski, Acta Phys. Polon. B3, 229 (1972).